Unassisted Segmentation of Multiple Retinal Layers via Spectral Rounding

D. Tolliver[1], Y. Koutis[1], H. Ishikawa[2,3], J.S. Schuman[2,3], G.L. Miller [1]

[1]Department of Computer Science, Carnegie Mellon University; [2]UPMC Eye Center, Eye and Ear Institute, Ophthalmology and Visual Science Research Center, Department of Ophthalmology, University of Pittsburgh School of Medicine, Pittsburgh, PA; [3]Dept. of Bioengineering, Swanson School of Engineering, University of Pittsburgh;

08-A-6017-ARVO

Carnegie Mellon School of Computer Science

Eye and Ear Institute, Department of Ophthalmology, University of Pittsburgh School of Medicine, Ophthalmology and Visual Sciences Research Center

UPMC Eye Center

Abstract

Purpose: To develop an automatic system to segment multiple retinal layers in three-dimensional spectral domain optical coherence tomography (3D SDOCT) images and to evaluate its performance in comparison with human assessment.

Methods: Spectral rounding, a graph partitioning image segmentation algorithm, was applied to weighted degree 4 lattice graphs constructed from 3D Cirrus OCT (Carl Zeiss Meditec, Inc., Dublin, CA) scan slices (200x200x1024 samplings in 6x6x2 mm centered). Intensity differences between adjacent pixels were computed to weight the lattice. Small magnitude eigenvectors of the resulting matrix representation, the normalized Laplacian of the graph, were calculated and used to determine probable boundary regions in the scan. The scans were automatically segregated into 5 regions, requiring 4 boundary detections.

Results: The proposed method successfully segregated the scans into 5 regions (Figure 1). The percentage of automatically detected boundary pixels within (+/- 5 pixels) of the human specified curves are given for the 4 boundaries, color-coded in the figures. The aggregate accuracy for the detected boundaries was 97.1% (red), 86.9% (green), 98.8% (blue), and 85.5% (yellow). These statistics were aggregated over 9 pathological subjects and 2 normative subjects - testing against hand segmentations of 4 randomly selected slices per case.

97%
86%
98%
85%

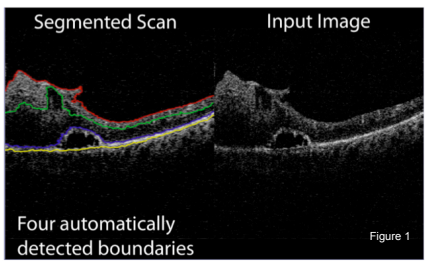

Figure 1

Conclusion: The graph theoretic model tracks complex boundary contours between anatomic ocular regions. This differs from conventional segmentation algorithms such as adaptive contours, which tend to fail in the presence of retinal pathology.

Introduction

- Segmentation provides a means of visualizing and measuring specific retinal layers in 3D spectral domain (SD-OCT) scans. Recently introduced, SD-OCT has an approximately 1.5 second scan time and provides a high resolution volumetric sample (e.g. 200x200x1024 samples).
- Unassisted segmentation would provide clinicians with easy access to new visualizations and potential clinical variables that respect the boundaries of retinal layers. Commercial SD-OCT software (Cirrus HD-OCT Software version 3.0, Carl Zeiss Meditec, Inc., Dublin, CA) has approached this problem by inferring the: internal limiting membrane (ILM), and retinal pigment epithelium (RPE). This method appears to use a low-order spline model to regularize the automatically fit curve. Such statistical models trade rigidity for fidelity an may fail to return segmentations of complex surfaces - such as those found in pathological cases (Figure 2).

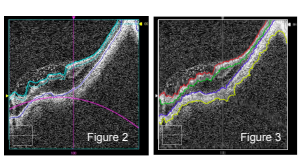

Figure 3: The red, green, blue, and yellow layers were automatically extracted from the inferred raw frame.

Note: the original image was not available for a comparison – an inferred raw image was reconstructed by removing colored pixels from the image and in-painting; the hard white lines where suppressed manually. The figure was produced by overlaying the segment boundaries on the reconstructed image.

- The purpose of this study was to test modern graph theoretic approaches to image segmentation on SD-OCT scans in order to assess the appropriateness of their application to Ophthalmological imaging data (Figure 3).

Financial disclosure: D. Tolliver, None; Y. Koutis, None; H. Ishikawa, None; J. Schuman, Alcon, F; Allergan, F; Carl Zeiss Meditec, Inc., F; Merck, F; Optoview, F; Heidelberg Engineering, F; Carl Zeiss Meditec, Inc., P; Alcon, R; Allergan, R; Carl Zeiss Meditec, Inc., R; Clarity, R; Merck, R; Heidelberg Engineering, R; G. L. Miller, None

Acknowledgement : NSF CCR-0635257; National Eye Institute (R01-EY01317-08, R01-EY11289-22 and P30-EY008098), AFOSR FA9550-040-1-0011; an unrestricted grant from Research to Prevent Blindness, and the Eye and Ear Foundation of Pittsburgh.

Method Description

- **Overview**: The algorithm consists of 3 primary steps: graph construction from SD-OCT scans, spectral rounding (which requires the calculation of eigenvectors of the normalized Laplacian), and recursive decomposition (which calls spectral rounding on the residual graph). The eigencalculation step consumes the majority of the computational resources and is addressed below.
- **Graph Construction**: the initial graph used in these experiments were constructed in either a 2 or 3 stage process. The first stage registers the 3D SD-OCT volume removing Z-axis and X-axis motion, after which a 3D median filter with (5 x 5 x 5) support is applied. Second, for a randomly selected slice, a matched quadrature-pair filterbank is applied to the slice image to detect zero crossings in the image intensities and determine an orientation robust edge magnitude (Figure 4). Third, a graph constructed from the edge feature images according to the following rule: $w(p,q) = exp((mag(p)-mag(q))^2/3)*abs(phase(p)-phase(q))$

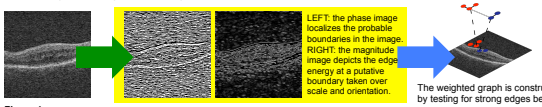

Figure 4

- **Spectral Rounding** iteratively updates an estimate of the bounding contour, by evaluating the eigenstructure of the associated graph Laplacian. This is accomplished by weakening the weights on heavily stretched edges in the graph. This stretch is measured as the difference in the eigenvector taken at neighboring pixels. In the visualization below low values are mapped to blue and high values are mapped to red, therefore a maximal stretch occurs between adjacent red and blue pixels.

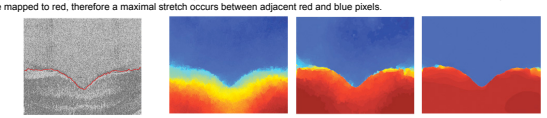

Recursive decomposition: after a boundary has been detected, the graph is restricted to those candidate pixels that contain the next layer to be segmented out. The segmentation results shown here require 4 cuts, one for each of the boundaries – the decomposition order was as follows: red, blue, green, yellow (note the green and yellow cuts may be performed in parallel as they are independent).

- **Computational Efficiency**: a novel eigensolver algorithm computes the required eigenstructure of the graph Laplacian. The algorithm[4] is mathematically robust and fully scalable: essentially a small number of CPU operations are performed for each pixel of the image, or voxel in a volume. The work can be split evenly among more than one CPUs when they available, for example in modern multi-core computers. Its full scalability ensures fast image segmentation and allowing real time user interaction, even on a standard desktop workstation.

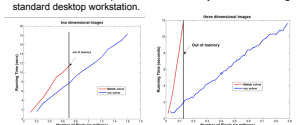

The computational core of our algorithm requires solutions f of the form: $Lf = \lambda Df$

where, L is the Laplacian (spring) matrix of the graph, D is the diagonal degree (mass) matrix, and f is an eigenvector – providing a map from the the pixels to the real numbers [see above for an example]. If we visualize the graph as a spring and mass system – with weak or strong springs connecting neighboring pixels – the eigenvectors can be thought of as the physical modes of vibration for the system. As eigenvectors are global functions of the graph traditional computational methods are impractical for image data.

Discussion:

- Analogously to 3D median filtering providing superior noise reduction when compared to 2D filtering – we believe substantial improvements in robustness and accuracy will come from direct 3D segmentation of SD-OCT scans.
  - Our current research is focused on applying our technology to 3D scans directly, as the graph theoretic model is essentially coordinate free – the same algorithm used to create the shown 2D results are directly applicable to 3D scans (see below for preliminary results).
- Reliable segmentation opens the possibility of clinical measurements based on the volume and shape statistics of the imaged structures – enhancing the set of inputs for computer assisted diagnoses.

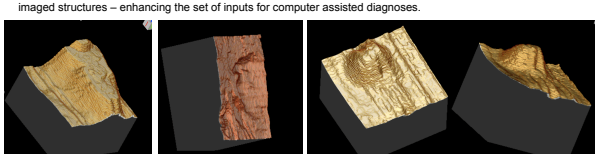

Results: no noise filtering or registration

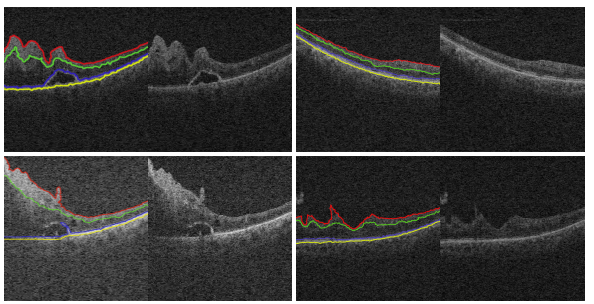

Results: thresholding, volumetric registration and 3D median filtering

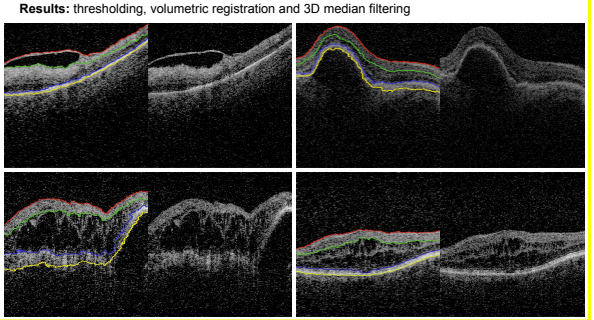

Results

- The proposed method successfully segregated the scans into 5 regions (Figure). The percentage of automatically detected boundary pixels within (+/- 5 pixels) of the human specified curves are given for the 4 boundaries, color-coded in the figures. The aggregate accuracy for the detected boundaries was 97.1% (red), 86.9% (green), 98.8% (blue), and 85.5% (yellow). These statistics were aggregated over 9 pathological subjects and 2 normative subjects - testing against hand segmentations of 4 randomly selected slices per case.
- The results above demonstrate the systems tolerance to the intricate contours induced by retinal pathologies. The upper collection contains segmentation results without registration or noise reduction. The second collection, boxed in yellow, contains results on slices with 3D median filtering and registration. All shown results are on scans taken of subjects with pathologies – as existing methods are believed to be reliable on normative subjects. *Note* the green and yellow contours are less constrained by the data and thus produce the lower prediction scores – an example of a failed segmentation can be seen in the yellow box, upper left hand corner.

References

3.Tolliver D, Miller GL. Spectral Rounding for Image Segmentation. Computer Vision and Pattern Recognition. 2006 July; 1(8): 435-542

4.Koutis Y, Miller G L. Graph partitioning into isolated, high conductance clusters: Theory, computation and applications to preconditioning [SPAA 08].

Contact: David Tolliver tolliver@cs.cmu.edu

NSF

UPMC University of Pittsburgh Medical Center

The Eye & Ear Foundation of Pittsburgh

SUPPORTED BY Research to Prevent Blindness